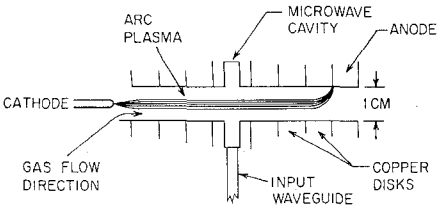

Fig. 1—Section of the plasma apparatus showing the microwave cavity.

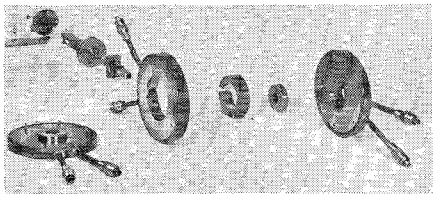

Fig. 2—Exploded view of the microwave cavity.

The mechanical complexity introduced by the requirements of water cooling and vacuability make the construction of separate cavities for each frequency undesirable. A single circular cylindrical cavity shell is described below which can by means of insert rings and plugs operate over a frequency range greater than 2 to 1 (36 to 88 Gc). The assembly has considerable mechanical strength. The cavity is short enough to avoid serious fluid flow problems but long enough to achieve a reasonable Q. Both the iris size and position can be changed to allow a variety of modes to be excited.

The cavity assembly is shown partially dismantled in Fig. 2. The cavity shell consists of three parts: a body 3 inches in diameter and 0.438 inch thick and two end plates each 3 inches in diameter and $\frac{5}{16}$ inch thick. All are copper with 0.5 per cent tellurium added for ease of machining. Copper provides both the high thermal conductivity and when polished the high surface electrical conductivity desired. Water channels milled in each part are connected via $\frac{3}{16}$ inch copper tubing to $\frac{1}{4}$ inch polyflow fittings. Each end plate is secured to the body by six screws which clamp a Parker 2-38 O-ring-vacuum seal. The actual microwave working surfaces are formed by an insert ring which reduces the diameter from 1.5 inches to that desired and two insert plugs which attach with screws to the end plates and fit inside the insert rings to reduce the length.

In the foreground of Fig. 2 one sees from right to left an end plate, insert plug, insert ring, cavity body, and the other end plate with insert plug attached. Behind is shown the waveguide which is built up to fit the rectangular hole in the body. The coupling iris is drilled in a 0.010 inch brass plate which is soldered directly onto the end of the input waveguide. This waveguide is inserted through the hole in the body, past the slotted ring until it seats against the plugs. A sliding flange shown mounted on the waveguide is then tightened down against a small O-ring (stretched over the waveguide). This arrangement affords a vacuum seal to the waveguide and also holds it in place. For nonsymmetrical excitation the waveguide is located as far off the cavity midplane as possible and the iris is moved off the guide center if necessary to obtain the appropriate coupling. While this scheme is not perfect it works well enough to allow excitation of TE_{nm2} modes with adequate coupling.

The theoretical Q_0 for the TE_{011} mode at 38 Gc (neglecting end plate holes) is about 7000. The experimental Q_0 is found to be greater than 2000. At some frequencies this exceeds the wavemeter Q used in spite of the cavity's large end plate holes and pancake shape. In the smallest cavity employed, the plasma need leap across a gap of only just over $\frac{1}{16}$ inch.

Data reproducibility is excellent. In actual use measurements were taken with the cavity. It was then dismantled and assembled with a different set of inserts. When it was reassembled in its original form, the original data were reproduced exactly (within experimental error).

WILLIAM T. MALONEY
Div. of Engrg. and Appl. Phys.
Harvard University
Cambridge, Mass.

Radiation Characteristics for a Magnetic Line Source in Homogeneous Electron Plasmas

The radiation characteristic of a magnetic line source in an anisotropic compressible electron plasma was discussed in a recent paper by Seshadri.[1] In Seshadri's paper an excessive amount of effort is devoted to evaluating certain integrals occurring in the Fourier transform solutions of the single-fluid magnetohydrodynamic equations. The following discussion presents a greatly simplified method of evaluating the appropriate integrals describing the "optical" and "plasma" modes of radiation.

The time harmonic (exp $-i\omega t$) equations for the single-fluid compressible system may be formulated as

$$\nabla \times \boldsymbol{E} - i\omega\mu_0 \boldsymbol{H} = -\boldsymbol{J}_m \tag{1}$$

$$\nabla \times \boldsymbol{H} + i\omega\epsilon_0 \boldsymbol{E} = Ne\boldsymbol{V} \tag{2}$$

$$-i\omega m N_0 \boldsymbol{V} = Ne(\boldsymbol{E} + \boldsymbol{V} \times \boldsymbol{B}_0) - \nabla P \tag{3}$$

$$a^2 m N_0 \nabla \doteq \boldsymbol{V} - i\omega P. \tag{4}$$

The notation utilized in (1)–(4) is that which Seshadri chose in his formulation. Furthermore, we now restrict our attention to a magnetic line source parallel to the y-axis of a right handed system (x, y, z). Imposing this constraint to (1)–(4) and applying Fourier transform theory, we obtain the integral equations for H_y and P (see Seshadri[2]).

$$H_y(x, z) = \frac{i\omega\epsilon_0 J_0}{4\pi^2\epsilon_1} \int_{-\infty}^{\infty}\int_{-\infty}^{\infty} \cdot \frac{(\eta^2 + \zeta^2 - k_a^2)e^{i(\zeta x + \eta z)}}{\Delta}\, d\eta d\zeta \tag{5}$$

$$P(x, z) = \frac{i\omega X B_0 \epsilon_0 \epsilon}{4\pi^2(1 - X)\epsilon_1} \int_{-\infty}^{\infty}\int_{-\infty}^{\infty} \cdot \frac{(\eta^2 + \zeta^2)e^{i(\zeta x + \eta z)}}{\Delta}\, d\eta d\zeta \tag{6}$$

where

$$X = \frac{\omega_p^2}{\omega^2}, \quad Y = \frac{\omega_g}{\omega}, \quad \epsilon = \epsilon_1^2 + \epsilon_2^2$$

$$\epsilon_1 = \frac{1 - X - Y^2}{1 - Y^2}, \quad \epsilon_2 = \frac{XY}{1 - Y^2},$$

$$\Delta = (\eta^2 + \zeta^2 - k_{mp}^2)(\eta^2 + \zeta^2 - k_{m0}^2) \cdot \left[\frac{(1 - X + Y)(1 - X - Y)}{(1 - X)(1 - X - Y^2)}\right],$$

k_{m0}^2 and k_{mp}^2 are roots of $P(\lambda) = 0$, where

$$P(\lambda) = \lambda^4 - (\omega^2/c^2 + \omega^2/a^2)(1 - X - Y^2) + (\omega^2/a^2)(\omega^2/c^2)[(1 - X)^2 - Y^2],$$

$$k_a^2 = \frac{\omega^2}{a^2}\left[\frac{(1 - X)^2 - Y^2}{1 - X}\right],$$

$$k_e^2 = \omega^2/c^2\left[\frac{(1 - X)^2 - Y^2}{1 - X - Y^2}\right].$$

Unfortunately, Seshadri chose to evaluate the integrals in (5) and (6) in rectangular coordinate systems as given. In so doing, he encountered multivalued integrands which complicated the evaluation of the magnetic field and hydrostatic pressure in the plasma. The following evaluation of the integrals provides a rather simple method for the description of the radiation characteristic of the line source.

The integrals are defined as

$$I_1 = \int_{-\infty}^{\infty}\int_{-\infty}^{\infty} \frac{(\eta^2 + \zeta^2 - k_a^2)e^{i(\zeta x + \eta z)}}{\Delta}\, d\eta d\zeta, \tag{7}$$

$$I_2 = \int_{-\infty}^{\infty}\int_{-\infty}^{\infty} \frac{(\eta^2 + \zeta^2)e^{i(\zeta x + \eta z)}}{\Delta}\, d\eta d\zeta. \tag{8}$$

Transforming both real-space and transform-space variables to polar coordinates, we recognize the integration with respect to the angular variable as an identity for the Bessel functions and obtain[3]

$$I_1(\rho) = 2\pi \int_0^{\infty} \frac{(\lambda^2 - k_a^2)\lambda J_0(\lambda\rho)d\lambda}{\Delta(\lambda)} \tag{9}$$

$$I_2(\rho) = 2\pi \int_0^{\infty} \frac{\lambda^3 J_0(\lambda\rho)d\lambda}{\Delta(\lambda)}. \tag{10}$$

We now make use of complex function theory, substitute Hankel functions for the

Manuscript received May 21, 1964; revised July 27, 1964.

[1] S. R. Seshadri, "Excitation of Plasma Waves in an Unbounded Homogeneous Plasma by a Line Source," IEEE TRANSACTIONS ON MICROWAVE THEORY AND TECHNIQUES, vol. MTT-11, pp. 39–49; January, 1963.

[2] *Ibid.*, see (35) and (36) on p. 43.

[3] E. Jahnke and F. Emde, "Tables of Functions," Dover Publications, New York, N. Y.; 1945.

Bessel functions and distort the contours of integration into the first and fourth quadrant of the complex λ-plane. Integrals involving $H_0^{(2)}(\lambda\rho)$ are evaluated in the fourth quadrant and those with $H_0^{(1)}(\lambda\rho)$ in the first quadrant. The integrals are then completely specified by the residues in the first and fourth quadrant.

However, we may simplify the evaluation by imposing the argument that there can be no poles in the fourth quadrant as such poles would generate space waves which would not satisfy the radiation condition as $\rho \to \infty$.[4] The integrals are then evaluated as

$$I_1(\rho) = 2\pi i \sum \text{Residues} \cdot \left[\frac{2\pi(\lambda^2 - k_a^2)\lambda H_0^{(1)}(\lambda\rho)}{2\Delta(\lambda)}\right]_{1st}, \quad (11)$$

$$I_2(\rho) = 2\pi i \sum \text{Residues} \cdot \left[\frac{2\pi\lambda^3 H_0^{(1)}(\lambda\rho)}{2\Delta(\lambda)}\right]_{4th} \quad (12)$$

The poles of the integrands in I_1 and I_2 are determined by the roots of $P(\lambda)$ given above. We find for the magnetic field and pressure the following expressions:

$$H_y(\rho) = \frac{\omega\epsilon_0\epsilon J_0}{4\epsilon_1(1-\beta)}\left\{\frac{(k_{mp}^2 - k_a^2)}{(k_{mp}^2 - k_{m0}^2)} H_0^{(1)}(k_{mp}\rho) + \frac{(k_{m0}^2 - k_a^2)}{(k_{m0}^2 - k_{mp}^2)} H_0^{(1)}(k_{mp}\rho)\right\}, \quad (13)$$

$$P(\rho) = \frac{B_0 X J_0}{4(1-X)} \frac{\omega\epsilon_0\epsilon}{\epsilon_1(1-\beta)} \cdot \left\{\frac{k_{mp}^2}{k_{mp}^2 - k_{m0}^2} H_0^{(1)}(k_{mp}\rho) + \frac{k_{m0}^2}{k_{m0}^2 - k_{mp}^2} H_0^{(1)}(k_{m0}\rho)\right\}. \quad (14)$$

The optical and plasma modes are described by the wave numbers k_{m0} and k_{mp} respectively. Assuming the velocity of sound is much less than the velocity of light ($a \ll c$) in the electron plasma, the wave numbers may be expressed as

$$k_{m0}^2 \doteq B(1 - \sqrt{1 - C/B^2}),$$

$$k_{mp}^2 \doteq B(1 + \sqrt{1 - C/B^2}). \quad (15)$$

where

$$2B = (\omega^2/a^2 + \omega^2/c^2)(1 - X - Y^2),$$

$$C = \frac{\omega}{a^2c^2}[(1-X)^2 - Y^2].$$

To discuss the propagation characteristics, we need only consider the range of values for the parameters X and Y. For this purpose we define the "parameter plane" defined with X and Y as coordinates. In this plane the critical curves are those for which $B=0$ and $C=0$. These curves are plotted in Fig. 1.

From this plot it is now a simple matter to determine the regions of the $X=Y$ plane

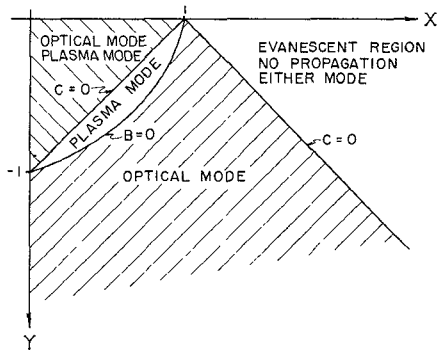

Fig. 1—Optical-plasma radiation characteristics.

in which the optical mode or the plasma mode are propagating or evanescent. Indeed one finds the modes propagate as illustrated in Fig. 1. The optical mode exhibits "cutoff" characteristics along the lines defined by $(1-X)^2 - Y^2 = 0$ and $1 - X - Y^2 = 0$. The plasma mode has only cutoff characteristics defined by $1 - X - Y^2 = 0$. It is now quite clear as to what values of parameters, X and Y, are critical in the excitation of radiation modes in a compressible plasma. Power splitting between the modes is now a relatively simple matter for the regions indicated in Fig. 1.

K. R. Cook
Dept. of Elec. Engrg.
Oklahoma State University
Stillwater, Okla.

Quasi-Optical Waveguide Filters

Oversize rectangular waveguide operating in the TE_{10} mode is useful in constructing components operating at millimeter and submillimeter wavelengths [1], [2]. This communication describes preliminary results on quasi-optical oversize waveguide filters. It is easier to construct filters using this technique and they have lower attenuation loss than conventional-size waveguide filters. When the waveguide is appreciably oversize (10 or more times standard-size TE_{10} waveguide), a good approximation to plane wave propagation exists. This enables gratings and dielectric slabs to be used in a way that is similar to their application in optical structures, which have previously been considered as filter-like elements at millimeter and submillimeter wavelengths [3], [4], [5]. We have examined the problems of making multi-element filters in oversize waveguide using the techniques of free-space optics modified appropriately for the oversize waveguide. We will describe in detail a two-port metallic grating and a four-port dielectric-slab filter.

A typical two-port band-pass metallic-grating structure can be constructed in oversize waveguide using quasi-optical techniques. The filter consists of n resonators, each resonator being q half wavelengths long. A typical grating consists of many regularly spaced iris holes in a flat metallic plate. Any coupling coefficient value can be obtained by choosing holes of the proper diameter.

The design theory for this filter, for the calculation of coupling susceptance, is similar to that for waveguide filters using standard-size waveguide except that standard coupling structures such as irises and slits cannot be used. To prevent higher modes from being produced, it is necessary to operate uniformly on the plane-wave front. Uniform operation is possible if the coupling is distributed throughout the surface that connects the two resonators. We have constructed and evaluated a filter of this type at 9 mm in a design that can be scaled to the submillimeter region.

This experimental two-resonator band-pass filter was designed in S-band waveguide. It operated at 32.775 Gc with a 22.5 Mc bandwidth and a 1.7 db insertion loss at its center frequency. Each resonator was five half-wavelengths long. A similar design in conventional waveguide (WR28 coin-silver waveguide) using a Q_u 60 per cent of theoretical, would have had a 6.6 db insertion loss. Fig. 1 shows the completed filter. The outer coupling holes are 0.104 inch in diameter and the inner holes are 0.053 inch in diameter. Each plate has 105 holes.

A graph of the insertion loss versus frequency for the oversize waveguide filter is shown in Fig 2. This figure also shows the insertion loss vs frequency characteristics at frequencies where each cavity was six half-wavelengths long. A scaled version is now under construction for operation at 330 Gc. In addition, we are studying quarter-wavelength dielectric-slab filters with similar characteristics.

A typical four-port dielectric-slab filter consists of a pair of parallel dielectric slabs, oriented at 45° in relation to the incident radiation, of thickness t, and separated by an air space d. This device couples power from port 1 to ports 2 and 4; no power is coupled to port 3, and port 1 is matched (Fig. 3).

The power transmitted from port 1 to port 2 is a function of d and λ. The multiple-slab structure can be used as a variable attenuator or as a directional coupler in addition to being used as a low-pass/high-pass filter. The preliminary evaluation and analysis of this filter has emphasized coupling properties (at a fixed frequency) with respect to the variation in d. The actual device was tested at 0.9 mm with a CSF carcinotron; it was far more practical to vary the slab separation than to vary the incident wavelength. The carcinotron was not operable over a wide enough bandwidth for meaningful testing nor could its frequency be determined very accurately. A theoretical analysis of the expected perfornance of the device was made for the single-frequency condition [1]. This analysis is readily modi-

[4] B. B. Baker and E. T. Copson, "The Mathematical Theory of Huygens' Principle," Oxford University Press, London, England; 1950.

Manuscript received June 1, 1964, revised July 21, 1964. The work reported here is based on a paper delivered at the 1964 PTGMTT Symposium, New York, N. Y. This work was supported in part by Rome Air Development Center, Griffiss Air Force Base, N. Y., under Contract AF 30(602)-2758.